

# Bayesian Restoration of Audio Degraded by Low-Frequency Pulses Modeled via Gaussian Process

Hugo T. de Carvalho, Flavio R. Avila, *Member, IEEE* and Luiz W. P. Biscainho, *Senior Member, IEEE*

**Abstract**—A common defect found when reproducing old vinyl and gramophone recordings with mechanical devices are the long pulses with significant low-frequency content caused by the interaction of the arm-needle system with deep scratches or even breakages on the media surface. Previous approaches to their suppression on digital counterparts of the recordings depend on a prior estimation of the pulse location, usually performed via heuristic methods. This paper proposes a novel Bayesian approach capable of jointly estimating the pulse location; interpolating the almost annihilated signal underlying the strong discontinuity that initiates the pulse; and also estimating the long pulse tail by a simple Gaussian Process, allowing its suppression from the corrupted signal. The posterior distribution for the model parameters as well for the pulse is explored via Markov-Chain Monte Carlo (MCMC) algorithms. Controlled experiments indicate that the proposed method, while requiring significantly less user intervention, achieves perceptual results similar to those of previous approaches and performs well when dealing with naturally degraded signals.

**Index Terms**—Audio restoration, Gaussian Process, Markov-Chain Monte Carlo, Bayesian inference.

## I. INTRODUCTION

A FAIRLY common degradation found in old vinyl and gramophone recordings are long pulses with significant low-frequency content produced by the nonlinear response of the arm-needle system of the playback device when it passes through a deep scratch or even a breakage on the surface of the respective media. More precisely, this degradation can be split into two complementary parts. An *initial discontinuity* that arises when the needle passes exactly over the physical damage is immediately followed by the *tail*, a low-frequency oscillation whose amplitude and frequency decay slowly. The discontinuity (lasting typically less than 10 ms) behaves as a high-variance noise added to the original signal that almost hides the underlying information, whereas the smooth tail (which in the most severe cases can be about 1-second long) is clearly superimposed to the original signal.

Since the physical restoration of the media is almost impossible, one must resort to numerical algorithms that process a digitized version of the degraded recording. A pioneering method tailored to tackle this type of degradation

was proposed in [1], [2]: it is based on the hypothesis of similarity among the pulses present in a signal, i.e., every physical damage found during reproduction is supposed to evoke a similar response of the system, differing only in location and amplitude. These two quantities are estimated by correlating the degraded signal with prototypical pulses of a reference database. The method achieves good results when this hypothesis is valid, but its scope is limited to pulses similar to the templates present in the database. Moreover, if two or more pulses overlap, it fails.

A statistical approach capable of dealing with more general cases can be found in [3], [4]. This method assumes that both the underlying signal and the pulse can be modeled by superimposed auto-regressive (AR) processes. The original signal is then estimated by separating the two processes. Some limitations are requiring the location of the pulse to be known and the unrealistic assumption about the AR model for the pulse.

In [5] a much simpler method is proposed, based on a nonlinear filtering technique called Two-Pass Split Window (TPSW). This filtering is employed to obtain a rough estimate of the pulse shape, which is then smoothed by a piecewise polynomial fitting. Although this method requires less computational power, the location of the pulse must be known in advance. In [6] the authors introduce a restoration method based on the Empirical Mode Decomposition, which decomposes a signal waveform into a set of simpler Intrinsic Mode Functions, but also requires the location of the pulse.

In general, the aforementioned methods only deal with the pulse tail, demanding also some de-clicking technique to interpolate the signal underlying the initial discontinuity. The exception is the AR separation based method [3], [4], which assumes that the initial discontinuity is modeled by the same AR process as the tail but with a higher excitation variance—a somewhat unrealistic hypothesis.

In [7], an innovative approach is introduced to jointly estimate the location of the pulse and restore the audio signal, including the excerpt underlying the initial discontinuity, that adopts a model for the pulse shape whose parameters are then estimated via Bayesian inference, by sampling from their posterior distribution. However, this method has three drawbacks, the first two being reconsidered in the present work: 1) the algorithm requires that several hyperparameters be manually tuned in order to correctly estimate the pulse tail parameters; 2) despite being capable of estimating precisely the location of the pulse, the method requires a good initialization; 3) the

The authors would like to thank CAPES, CNPq, and FAPERJ agencies for funding their research work.

Hugo T. de Carvalho and Luiz W. P. Biscainho are with the Federal University of Rio de Janeiro (UFRJ), Rio de Janeiro, Brazil (e-mail: hugo@dme.ufrj.br, wagner@smt.ufrj.br).

Flavio R. Avila is with Rio de Janeiro State University, Rio de Janeiro 20550-900, Brazil. (e-mail: flavio.avila@uerj.br)

method is not capable of dealing with superimposed pulses, because in this scenario the posterior distributions become very complicated to handle, even in the context of Markov-Chain Monte Carlo methods.

This work introduces an improvement of the method proposed in [7] that circumvents the first two issues above: 1) the pulse tail is modeled via a Gaussian Process, requiring much less hyperparameters to be tuned; 2) an efficient initialization procedure based on [8] is adopted, which provides good initial estimates of both location and duration of the initial discontinuity. But even if the posterior distribution does not increase in complexity in the case of overlapping pulses thanks to the Gaussian Process modeling of the pulse tail, the problem of estimating the underlying signal when a new initial discontinuity is superimposed to an unfinished tail still requires further investigation.

The paper is organized as follows: after this Introduction, Section II recalls the shape-based model for the pulse and introduces the proposed Gaussian Process model for the pulse tail, followed by a brief presentation of the AR model assumed for the underlying signal in Section III; Section IV briefly describes the sampling algorithm employed, followed by the computation of the marginal likelihood in Section V, and by the computation of the conditional distributions and description of the sampling procedures in Section VI; results are presented in Section VII, and conclusions are drawn in Section VIII.

## II. A MODEL FOR THE DEGRADATION

As already mentioned, a single pulse of the type considered in this work can be described by two contiguous parts: the initial discontinuity (when the needle passes through the physical degradation) and the tail (dumped oscillations of decaying frequency due to the non-linear response of the playback device to the impulsive excitation). These two parts of the degradation are denoted, respectively, by vectors  $\mathbf{v}_d$  and  $\mathbf{v}_t$ . When necessary, a superscript “s” or “G” will be added to vector  $\mathbf{v}_t$  in order to make explicit whether the shape-based or the Gaussian Process model is being used, respectively. There is no superscript when this distinction is not necessary.

Assuming the audio signal is processed in time frames of length  $N$ , denote the corresponding original and corrupted signal blocks by  $\mathbf{x}$  and  $\mathbf{y}$ , respectively. In order to describe the relationship between these vectors and the degradation in vectors  $\mathbf{v}_d$  and  $\mathbf{v}_t$ , three sets of indexes are defined:  $\mathbf{i}_0$ ,  $\mathbf{i}_1$  and  $\mathbf{i}_2$ , indicating the time samples in  $\mathbf{y}$  that belong to the region preceding the degradation, to the initial discontinuity, and to the tail, respectively. Sub-vectors  $\mathbf{x}_0$ ,  $\mathbf{y}_0$ ,  $\mathbf{x}_1$ ,  $\mathbf{y}_1$ ,  $\mathbf{x}_2$ , and  $\mathbf{y}_2$  contain the time samples corresponding to their respective sets of indexes, such that

$$\mathbf{y}_0 = \mathbf{x}_0, \quad (1)$$

$$\mathbf{y}_1 = \mathbf{x}_1 + \mathbf{v}_d, \quad (2)$$

$$\mathbf{y}_2 = \mathbf{x}_2 + \mathbf{v}_t. \quad (3)$$

By defining the set of auxiliary matrices  $\mathbf{K}$ ,  $\mathbf{U}_1$ , and  $\mathbf{U}_2$ , containing the columns of an  $N \times N$  identity matrix indexed by  $\mathbf{i}_0$ ,  $\mathbf{i}_1$ , and  $\mathbf{i}_2$ , respectively, one can write

$$\mathbf{x} = \mathbf{K}\mathbf{x}_0 + \mathbf{U}_1\mathbf{x}_1 + \mathbf{U}_2\mathbf{x}_2. \quad (4)$$

In the following, the models for the initial discontinuity and the tail of the pulse are described.

### A. Initial discontinuity

The initial discontinuity, stored in vector  $\mathbf{v}_d$ , can be modeled by Gaussian white noise superimposed to the underlying original signal in vector  $\mathbf{x}_1$ . This part of the pulse begins at sample  $n_0$  and lasts for  $M$  samples, with fixed variance  $\sigma_d^2$ :

$$\mathbf{v}_d(n) = r(n)[u(n - n_0) - u(n - n_0 - M)], \quad (5)$$

where  $u(n)$  is the unit step function,  $r(n) \sim \mathcal{N}(0, \sigma_d^2)$ , and  $n_0$ ,  $M$ , and  $\sigma_d^2$  are unknown. These three parameters are more concisely denoted by vector  $\boldsymbol{\theta}_d = [n_0 \ M \ \sigma_d^2]^T$ .

### B. Shape-based model for the tail

Here the model adopted in [7] for the tail is briefly recalled. Based on [5], it is mathematically described by

$$\mathbf{v}_t^s(n) = V_t e^{-n/(f'\tau_m)} \sin\left(2\pi n \frac{f_n}{f'} + \phi\right) \times [u(n - n_0 - M - 1)], \quad (6)$$

where

$$f_n = (f_{\max} - f_{\min})e^{-n/(f'\tau_f)} + f_{\min}. \quad (7)$$

This model is motivated by visual inspection of pulses present in silent parts of degraded audio signals [3], which exhibit a similar behavior: a decay in amplitude described by the exponential function, a decay in frequency modeled by variable  $f_n$  inside the sinusoidal function. Variables  $n_0$  and  $M$  are defined as before, and the remaining ones are precisely defined below:

- $V_t$  is related to the tail amplitude;
- $f'$  is the signal sampling rate (usually 44.1 kHz);
- $\tau_m$  is the time constant (in seconds) associated with the pulse envelope decay;
- $\tau_f$  is the time constant (in seconds) associated with the pulse frequency decay;
- $f_{\max}$  and  $f_{\min}$  are, respectively, the maximum and minimum tail oscillation frequencies (in Hz);
- $\phi$  is the initial phase of the pulse.

All these quantities (except for  $f'$ ) are also unknown beforehand. Let vector  $\boldsymbol{\theta}_t^s = [V_t \ \tau_m \ \tau_f \ f_{\max} \ f_{\min} \ \phi]^T$  store such tail parameters. They can be visualized in Figure 1, where a prototypical pulse that follows the model above is depicted.

### C. Gaussian Process model for the tail

Gaussian Processes are a widely employed technique in Statistics, Machine Learning and Linear Regression [9], [10], [11]. Before presenting its application to the current problem, some important facts should be recalled. A stochastic process  $\mathbf{G} = \{G_t\}_{t \in \mathcal{T}}$ , indexed by some set  $\mathcal{T}$ , is said to be a Gaussian Process if for any finite subset  $\{t_1, \dots, t_n\} \in \mathcal{T}$ , the joint

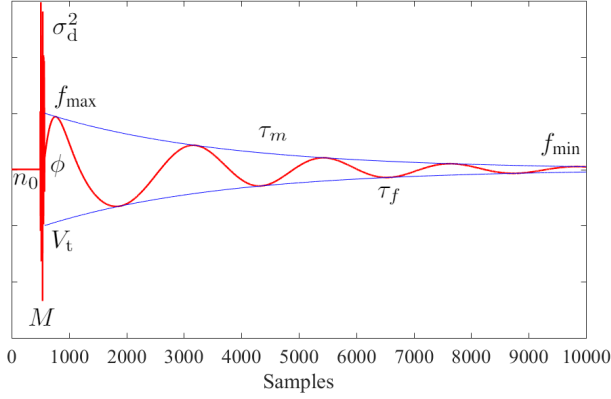


Fig. 1. Model for the pulse shape following Equation 6.

distribution of the random vector  $(G_{t_1}, \dots, G_{t_n})$  is Gaussian. Note that Gaussian distributions are completely determined by their first and second order statistics, so by assuming (without loss of generality) zero mean, several features of the process are encoded in its *covariance kernel*, denoted by  $K(t, t')$ , for  $t, t' \in \mathcal{T}$ . This function describes the dependence between any two random variables (i.e. time instants) of the process, and there are several commonly used covariance kernels tailored to impose some desired structure, like stationarity, smoothness, and periodicity, among others [12]. For a detailed discussion about Gaussian processes, see [10]. The fact that  $\mathbf{G}$  is a Gaussian Process with zero mean and covariance kernel  $K$  is concisely denoted by the expression

$$\mathbf{G} \sim \mathcal{GP}(0, K). \quad (8)$$

Returning to the modeling of the pulse tail, stored in vector  $\mathbf{v}_t$ , it can be seen as a generic function superimposed to the underlying signal in vector  $\mathbf{x}_2$ . This function is assumed to be much smoother than the underlying signal, and this assumption was implicitly taken into account in the design of the shape-based model. In order to give more flexibility to the pulse tail description, the deterministic function is replaced by a sample from a Gaussian Process with a squared-exponential covariance kernel given by

$$K_{SE}(t, t') = \sigma_f^2 \exp\left(-\frac{|t - t'|^2}{2\sigma_\ell^2}\right), \quad (9)$$

i.e.,  $\mathbf{v}_t^G \sim \mathcal{GP}(0, K_{SE})$ . Parameters  $\sigma_f$  and  $\sigma_\ell$  control the amplitude of the pulse and the effective extent of the covariance kernel, respectively.

The choice of this covariance kernel to model the tail of a long pulse is arguable, since it models a stationary process, which is clearly not the case of the typical pulse tail. A more precise model would require the definition of a covariance kernel specific to this application, with some additional parameters to encode the desired behavior. The drawback of such a choice would be to excessively increase the model complexity. The good results obtained with the squared-exponential covariance kernel consolidate our option for simplicity.

Now, in this framework, in addition to the parameters  $\sigma_f^2$  and  $\sigma_\ell^2$  of the covariance kernel, the whole vector  $\mathbf{v}_t^G$

containing the tail of the pulse must be estimated. Such quantities are assembled in vector

$$\boldsymbol{\theta}_t^G = [(\mathbf{v}_t^G)^T \ \sigma_f^2 \ \sigma_\ell^2]^T. \quad (10)$$

### III. A MODEL FOR THE UNDERLYING SIGNAL

In the context of audio restoration it is common to model the underlying original signal, here denoted by  $\mathbf{x}$ , as an autoregressive (AR) process of fixed order  $P$  [3]. More precisely, the samples of signal  $\mathbf{x}$  satisfy the following difference equation:

$$x(n) = \sum_{i=1}^P a_i x(n-i) + e(n), \quad (11)$$

where  $e(n)$  is the innovation error, modeled as a white Gaussian noise with variance  $\sigma_e^2$ . This model is an easy way to encode the predictability of audio signals in a short scale together with some unpredictable relation between successive samples. From the signal processing viewpoint, Equation (11) describes signal  $\mathbf{x}$  as the output of an all-pole linear filter whose input is signal  $\mathbf{e} = [e(1) \ \dots \ e(N)]^T$ , with transfer function given by

$$A(z) = \frac{1}{1 - \sum_{i=1}^P a_i z^{-i}}. \quad (12)$$

Therefore, the coefficients in vector  $\mathbf{a}$  are related to the most prominent frequencies in signal  $\mathbf{x}$ , through the poles of function  $A(z)$ .

It is important to discuss how long the block under analysis can be in order to be accurately described by an AR model. A reasonable choice is the time interval during which  $\mathbf{x}$  can be considered stationary, which for audio signals is usually accepted as around 20 ms (approximately 1,000 samples at a frequency sampling rate of 44,100 Hz, for instance). However, as mentioned before, the overall pulse duration can be much longer. The most natural way to deal with this issue would be to split signal  $\mathbf{x}$  into contiguous blocks of approximately 20 ms each and describe each of them with the corresponding AR model. However, this choice would greatly increase the complexity of the method.

The solution proposed here is to model the original signal immediately preceding the degradation and during the initial discontinuity, i.e. vector  $[\mathbf{x}_0^T \ \mathbf{x}_1^T]^T$ , by a single AR model of order about 40; and during the pulse tail, i.e. vector  $\mathbf{x}_2$ , as white Gaussian noise (a degenerated AR model of order zero). This apparent oversimplification can be justified: since by hypothesis the pulse tail is much smoother than the underlying signal and consists essentially of low frequency content, in the large time-scale of the tail the signal is almost indistinguishable from white noise. Notice that a high-order AR model must be kept for the first part, since this information will be crucial to restore the virtually missed  $\mathbf{x}_1$ .

An additional simplification can be made: since estimating the coefficients of the AR model together with the other parameters would make the computational time very large, they are estimated from  $\mathbf{y}_0$ , the region preceding the degradation, and kept constant through the whole procedure. This

approximation is justifiable, since these parameters will only be used to estimate  $\mathbf{x}_1$ , the signal underlying the initial discontinuity. Being  $\mathbf{y}_0 = \mathbf{x}_0$  and contiguous to  $\mathbf{x}_1$ , it is reasonable to assume they follow the same AR model.

We denote the coefficients of the AR model by  $\mathbf{a} = [a_1 \dots a_P]^T$ , which, together with  $\sigma_e^2$ , form vector

$$\boldsymbol{\theta}_x = [\mathbf{a}^T \ \sigma_e^2]^T \quad (13)$$

containing all parameters that model the underlying signal.

As discussed in [3], [7], since the distribution of the innovation error  $\mathbf{e}$  is Gaussian, by a simple change of variables one is able to write the distribution for  $\mathbf{x}$  as

$$p(\mathbf{x}|\boldsymbol{\theta}_x) = \frac{1}{(2\pi\sigma_e^2)^{\frac{(N-P)}{2}}} \exp\left(-\frac{1}{2\sigma_e^2}\mathbf{x}^T\mathbf{A}^T\mathbf{A}\mathbf{x}\right), \quad (14)$$

where matrix  $\mathbf{A}$  is given by

$$\mathbf{A} = \begin{bmatrix} -a_P & \dots & -a_1 & 1 & 0 & \dots & 0 \\ 0 & -a_P & \dots & -a_1 & 1 & \ddots & \vdots \\ \vdots & \ddots & \ddots & \ddots & \ddots & \ddots & \vdots \\ 0 & \dots & 0 & -a_P & \dots & -a_1 & 1 \end{bmatrix}. \quad (15)$$

Auxiliary matrices  $\mathbf{A}_0$ ,  $\mathbf{A}_1$  and  $\mathbf{A}_2$  contains the columns of  $\mathbf{A}$  indexed by  $\mathbf{i}_0$ ,  $\mathbf{i}_1$  and  $\mathbf{i}_2$ , respectively.

#### IV. DESCRIPTION OF THE ALGORITHM

Firstly, assume that vector  $\boldsymbol{\theta}_x$ , as discussed in Section III, has been estimated beforehand and kept constant through the entire procedure. At this point, the goal is to recover the underlying signal  $\mathbf{x}$  from the observed degraded signal  $\mathbf{y}$ . This can be achieved by estimating the auxiliary quantities stored in vectors  $\boldsymbol{\theta}_d$  and  $\boldsymbol{\theta}_t$ —the latter related to either the shape-based or the Gaussian Process model for the pulse tail. Assuming that the original signal is well described by an AR model, it is possible to obtain after some manipulation the likelihood  $p(\mathbf{y}|\mathbf{x}, \boldsymbol{\theta}_x, \boldsymbol{\theta}_d, \boldsymbol{\theta}_t)$ . Bayes' Theorem leads to the posterior distribution of the desired quantities

$$p(\mathbf{x}, \boldsymbol{\theta}_d, \boldsymbol{\theta}_t | \boldsymbol{\theta}_x, \mathbf{y}). \quad (16)$$

Since this expression is analytically intractable, this distribution is sampled from via the Gibbs sampler [13], [14], [15] (eventually with some Metropolis steps if the corresponding conditional distribution is not from a known family of distributions), implemented as follows:

a) Initialize values  $n_0^{(0)}$ ,  $M^{(0)}$ ,  $\sigma_d^{2(0)}$ ,  $\boldsymbol{\theta}_t^{(0)}$  and  $\mathbf{x}^{(0)}$ .

b) For  $k$  from 1 to  $N_{\text{iter}}$ :

i) Sample  $n_0^{(k)}$  and  $M^{(k)}$  from distribution

$$p(n_0, M | \sigma_d^{2(k-1)}, \boldsymbol{\theta}_t^{(k-1)}, \mathbf{x}^{(k-1)}, \boldsymbol{\theta}_x, \mathbf{y}).$$

ii) Sample  $\boldsymbol{\theta}_t^{(k)}$  and  $\mathbf{x}^{(k)}$  from distribution

$$p(\boldsymbol{\theta}_t, \mathbf{x} | n_0^{(k)}, M^{(k)}, \sigma_d^{2(k-1)}, \boldsymbol{\theta}_x, \mathbf{y}).$$

iii) Sample  $\sigma_d^{2(k)}$  from distribution

$$p(\sigma_d^2 | n_0^{(k)}, M^{(k)}, \boldsymbol{\theta}_t^{(k)}, \mathbf{x}^{(k)}, \boldsymbol{\theta}_x, \mathbf{y}).$$

Variables  $n_0$  and  $M$  are jointly sampled since block Gibbs sampling is empirically known to improve the convergence

speed of the algorithm [16]; the joint sampling of  $\boldsymbol{\theta}_t$  and  $\mathbf{x}$  is adopted for the same reason, in addition to the fact that their joint distribution can be rewritten, via Bayes' Theorem, in the following form, which will simplify some computations in Section V:

$$p(\boldsymbol{\theta}_t, \mathbf{x} | \boldsymbol{\theta}_d, \boldsymbol{\theta}_x, \mathbf{y}) = p(\boldsymbol{\theta}_t | \boldsymbol{\theta}_d, \boldsymbol{\theta}_x, \mathbf{y}) p(\mathbf{x} | \boldsymbol{\theta}_t, \boldsymbol{\theta}_d, \boldsymbol{\theta}_x, \mathbf{y}) \propto [p(\mathbf{y} | \boldsymbol{\theta}_t, \boldsymbol{\theta}_d, \boldsymbol{\theta}_x) p(\boldsymbol{\theta}_t)] p(\mathbf{x} | \boldsymbol{\theta}_t, \boldsymbol{\theta}_d, \boldsymbol{\theta}_x, \mathbf{y}). \quad (17)$$

The order of the sampling is quite arbitrary, since it does not affect the convergence properties of the algorithm [16]. This particular order was implemented since it seems more natural to first sample  $n_0$  and  $M$ , the pulse location variables, and then sample the other variables. Finally, the mean of the posterior distribution, estimated by averaging the samples obtained after the burn-in time, is used to perform the restoration procedure.

Notice that the sampling of  $\boldsymbol{\theta}_t$  depends on the considered model. For the shape-based model, the posterior distribution  $p(\boldsymbol{\theta}_t^s | \mathbf{x}, \boldsymbol{\theta}_d, \boldsymbol{\theta}_x, \mathbf{y})$  is very complicated and does not belong to any known family of distributions; therefore, in this case, a Metropolis-Hastings step is performed within the Gibbs sampler—for more details, see [7]. Hereafter, the focus will be on the computation of the Gaussian Process model only, detailing the derivation of each conditional distribution of interest. For the sake of completeness, the corresponding results for the shape-based model are also reported.

#### V. COMPUTATION OF THE MARGINAL LIKELIHOOD

This section develops the marginal likelihood  $p(\mathbf{y} | \boldsymbol{\theta}_t, \boldsymbol{\theta}_d, \boldsymbol{\theta}_x)$ , which will be needed later.

Firstly, two important results about Gaussian distributions must be recalled [3].

- Consider an integral of the form

$$I = \int_{\mathbb{R}^D} \exp\left\{-\frac{1}{2}(a + \mathbf{b}^T \mathbf{z} + \mathbf{z}^T \mathbf{C} \mathbf{z})\right\} d\mathbf{z}. \quad (18)$$

Since the term inside the exponential function is a quadratic form on  $\mathbf{z}$ , one could complete the squares and compare the obtained expression with the probability density function of a multivariate Gaussian. One can then prove that [3]

$$I = \frac{(2\pi)^{D/2}}{\det(\mathbf{C})^{1/2}} \exp\left\{-\frac{1}{2}\left(a - \frac{\mathbf{b}^T \mathbf{C}^{-1} \mathbf{b}}{4}\right)\right\}. \quad (19)$$

- Now, consider the product of two multivariate Gaussian probability density functions, that is,

$$f(\mathbf{z}) = f_1(\mathbf{z}) f_2(\mathbf{z}), \quad (20)$$

where  $f_1(\mathbf{z}) = \mathcal{N}(\mathbf{z} | \boldsymbol{\mu}_1, \boldsymbol{\Sigma}_1)$  and  $f_2(\mathbf{z}) = \mathcal{N}(\mathbf{z} | \boldsymbol{\mu}_2, \boldsymbol{\Sigma}_2)$ . Also after completing the squares inside the exponentials, one is able to prove that  $f(\mathbf{z})$  is also the probability density function of a multivariate Gaussian distribution, but with covariance matrix given by  $\boldsymbol{\Sigma} = (\boldsymbol{\Sigma}_1^{-1} + \boldsymbol{\Sigma}_2^{-1})^{-1}$  and mean  $\boldsymbol{\mu} = \boldsymbol{\Sigma}^{-1}(\boldsymbol{\Sigma}_1^{-1} \boldsymbol{\mu}_1 + \boldsymbol{\Sigma}_2^{-1} \boldsymbol{\mu}_2)$ .

Proceeding to the derivation of the marginal likelihood, it can be rewritten as

$$p(\mathbf{y} | \boldsymbol{\theta}_t, \boldsymbol{\theta}_d, \boldsymbol{\theta}_x) = \int_{\mathbb{R}^N} p(\mathbf{x}, \mathbf{y} | \boldsymbol{\theta}_t, \boldsymbol{\theta}_d, \boldsymbol{\theta}_x) d\mathbf{x} = \int_{\mathbb{R}^N} p(\mathbf{x} | \boldsymbol{\theta}_t, \boldsymbol{\theta}_d, \boldsymbol{\theta}_x) p(\mathbf{y} | \mathbf{x}, \boldsymbol{\theta}_t, \boldsymbol{\theta}_d, \boldsymbol{\theta}_x) d\mathbf{x}. \quad (21)$$

Notice that  $\mathbf{x}$  does not depend on  $\boldsymbol{\theta}_d$  and  $\boldsymbol{\theta}_t$ , since both sets of parameters describe only the degradation, and not the underlying original signal. Therefore,  $p(\mathbf{x}|\boldsymbol{\theta}_t, \boldsymbol{\theta}_d, \boldsymbol{\theta}_x)$  can be replaced with  $p(\mathbf{x}|\boldsymbol{\theta}_x)$ , which from Equation (14) is Gaussian with mean  $\mathbf{0}$  and covariance matrix  $\sigma_e^2(\mathbf{A}^T \mathbf{A})^{-1}$ . To compute  $p(\mathbf{y}|\mathbf{x}, \boldsymbol{\theta}_t, \boldsymbol{\theta}_d, \boldsymbol{\theta}_x)$ , notice first that the time samples in  $\mathbf{y}_0$  are uncorrupted, and the time samples in  $\mathbf{y}_2$  depends only on the content of  $\boldsymbol{\theta}_t$ ; therefore, their distributions can be modeled by adequate multi-dimensional Dirac's delta distributions. Moreover, the time samples in  $\mathbf{y}_1$  are the time samples in  $\mathbf{x}_1$  with additive white Gaussian noise. Therefore,

$$p(\mathbf{y}|\mathbf{x}, \boldsymbol{\theta}_t, \boldsymbol{\theta}_d, \boldsymbol{\theta}_x) = \delta(\mathbf{y}_0 - \mathbf{x}_0) \mathcal{N}(\mathbf{y}_1|\mathbf{x}_1, \sigma_d^2 \mathbf{I}_M) \delta(\mathbf{y}_2 - (\mathbf{x}_2 + \mathbf{v}_t)), \quad (22)$$

and

$$p(\mathbf{x}, \mathbf{y}|\boldsymbol{\theta}_t, \boldsymbol{\theta}_d, \boldsymbol{\theta}_x) = \mathcal{N}(\mathbf{x}|\mathbf{0}, \sigma_e^2(\mathbf{A}^T \mathbf{A})^{-1}) \times [\delta(\mathbf{y}_0 - \mathbf{x}_0) \mathcal{N}(\mathbf{y}_1|\mathbf{x}_1, \sigma_d^2 \mathbf{I}_M) \delta(\mathbf{y}_2 - (\mathbf{x}_2 + \mathbf{v}_t))]. \quad (23)$$

Notice that the integral in Equation (21) is calculated with respect to  $\mathbf{x}$ , and the second Gaussian in Equation (23) depends on  $\mathbf{x}_1$  only via its mean. In order to make explicit the dependence on  $\mathbf{x}_1$ , one can use the symmetry of the Gaussian distribution and the fact that  $\mathcal{N}(\mathbf{y}_1|\mathbf{x}_1, \sigma_d^2 \mathbf{I}_M) = \mathcal{N}(\mathbf{x}_1|\mathbf{y}_1, \sigma_d^2 \mathbf{I}_M)$  (i.e., both PDFs have the same formula). Using the decomposition of  $\mathbf{x}$  given in Equation (4):

$$p(\mathbf{x}, \mathbf{y}|\boldsymbol{\theta}_t, \boldsymbol{\theta}_d, \boldsymbol{\theta}_x) = \mathcal{N}(\mathbf{K}\mathbf{x}_0 + \mathbf{U}_1\mathbf{x}_1 + \mathbf{U}_2\mathbf{x}_2|\mathbf{0}, \sigma_e^2(\mathbf{A}^T \mathbf{A})^{-1}) \times [\delta(\mathbf{y}_0 - \mathbf{x}_0) \mathcal{N}(\mathbf{x}_1|\mathbf{y}_1, \sigma_d^2 \mathbf{I}_M) \delta(\mathbf{y}_2 - (\mathbf{x}_2 + \mathbf{v}_t))], \quad (24)$$

and finally,

$$p(\mathbf{y}|\boldsymbol{\theta}_t, \boldsymbol{\theta}_d, \boldsymbol{\theta}_x) = \int_{\mathbb{R}^N} \mathcal{N}(\mathbf{K}\mathbf{x}_0 + \mathbf{U}_1\mathbf{x}_1 + \mathbf{U}_2\mathbf{x}_2|\mathbf{0}, \sigma_e^2(\mathbf{A}^T \mathbf{A})^{-1}) \times [\delta(\mathbf{y}_0 - \mathbf{x}_0) \mathcal{N}(\mathbf{x}_1|\mathbf{y}_1, \sigma_d^2 \mathbf{I}_M) \delta(\mathbf{y}_2 - (\mathbf{x}_2 + \mathbf{v}_t))] d\mathbf{x} = \int_{\mathbb{R}^M} \mathcal{N}(\mathbf{K}\mathbf{y}_0 + \mathbf{U}_1\mathbf{x}_1 + \mathbf{U}_2(\mathbf{y}_2 - \mathbf{v}_t)|\mathbf{0}, \sigma_e^2(\mathbf{A}^T \mathbf{A})^{-1}) \times \mathcal{N}(\mathbf{x}_1|\mathbf{y}_1, \sigma_d^2 \mathbf{I}_M) d\mathbf{x}_1. \quad (25)$$

The integral can be computed by using the Gaussian PDFs along with the results in the beginning of this Section with  $\mathbf{z} = \mathbf{x}_1$ :

$$p(\mathbf{y}|\boldsymbol{\theta}_t, \boldsymbol{\theta}_d, \boldsymbol{\theta}_x) = \frac{\lambda^M}{(2\pi\sigma_e^2)^{\frac{N-P}{2}} \det(\boldsymbol{\Phi})} \exp\left\{-\frac{E_{\min}}{2\sigma_e^2}\right\}, \quad (26)$$

where

$$\begin{aligned} E_{\min} &= \lambda^2 \mathbf{y}_1^T \mathbf{y}_1 + \mathbf{z}^T \begin{bmatrix} \mathbf{A}_0^T \\ \mathbf{A}_2^T \end{bmatrix} [\mathbf{A}_0 \ \mathbf{A}_2] \mathbf{z} + (\mathbf{x}_1^{\text{MAP}})^T \boldsymbol{\Theta}, \\ \mathbf{z} &= \begin{bmatrix} \mathbf{y}_0 \\ \mathbf{y}_2 - \mathbf{v}_t \end{bmatrix}, \\ \mathbf{x}_1^{\text{MAP}} &= \boldsymbol{\Phi}^{-1} \boldsymbol{\Theta}, \\ \boldsymbol{\Phi} &= \lambda \mathbf{I}_M + \mathbf{A}_1^T \mathbf{A}_1, \\ \boldsymbol{\Theta} &= \lambda \mathbf{y}_1 - \mathbf{A}_1^T [\mathbf{A}_0 \ \mathbf{A}_2] \mathbf{z}, \\ \lambda &= \sigma_e^2 / \sigma_d^2. \end{aligned} \quad (27)$$

This expression can be simplified by noting that  $\lambda$  is likely to be very small, since  $\sigma_d^2$  is usually several orders of magnitude greater than  $\sigma_e^2$ . In the argument of the exponential in Equation (26) this quantity multiplies  $\mathbf{y}_1$ , whose entries do not typically exceed  $3\sigma_d$  beyond the underlying signal, due to their Gaussian distribution. One can then ignore all terms involving  $\lambda$  inside the exponential in Equation (26), which becomes proportional to  $\exp(-\frac{1}{2} \mathbf{z}^T \mathbf{R} \mathbf{z})$ , where

$$\mathbf{R} = \frac{1}{\sigma_e^2} \begin{bmatrix} \mathbf{A}_0^T \\ \mathbf{A}_2^T \end{bmatrix} \mathbf{S} [\mathbf{A}_0 \ \mathbf{A}_2], \quad (28)$$

with

$$\mathbf{S} = \mathbf{I}_{N-P} - \mathbf{A}_1 (\mathbf{A}^{-1} \mathbf{A})^{-1} \mathbf{A}_1^T. \quad (29)$$

In several steps of the algorithm the distribution  $p(\mathbf{x}|\boldsymbol{\theta}_t, \boldsymbol{\theta}_d, \boldsymbol{\theta}_x, \mathbf{y})$ , which was indirectly obtained above, will be necessary. Notice that, by Bayes' Theorem,

$$\begin{aligned} p(\mathbf{x}|\boldsymbol{\theta}_t, \boldsymbol{\theta}_d, \boldsymbol{\theta}_x, \mathbf{y}) &\propto p(\mathbf{y}|\boldsymbol{\theta}_t, \boldsymbol{\theta}_d, \boldsymbol{\theta}_x, \mathbf{x}) p(\mathbf{x}|\boldsymbol{\theta}_t, \boldsymbol{\theta}_d, \boldsymbol{\theta}_x) = \\ &= p(\mathbf{y}|\boldsymbol{\theta}_t, \boldsymbol{\theta}_d, \boldsymbol{\theta}_x, \mathbf{x}) p(\mathbf{x}|\boldsymbol{\theta}_x) = \\ &= [\delta(\mathbf{y}_0 - \mathbf{x}_0) \mathcal{N}(\mathbf{x}_1|\mathbf{y}_1, \sigma_d^2 \mathbf{I}_M) \delta(\mathbf{y}_2 - (\mathbf{x}_2 + \mathbf{v}_t))] \times \\ &\quad \mathcal{N}(\mathbf{K}\mathbf{x}_0 + \mathbf{U}_1\mathbf{x}_1 + \mathbf{U}_2\mathbf{x}_2|\mathbf{0}, \sigma_e^2(\mathbf{A}^T \mathbf{A})^{-1}), \end{aligned} \quad (30)$$

as obtained in Equation (24). This expression can be further simplified by noting that the second Gaussian depends essentially only on  $\mathbf{x}_1$ , since its dependence on  $\mathbf{x}_0$  and  $\mathbf{x}_2$  is defined by the two Dirac's deltas. After using again the fact that a product of Gaussians is also Gaussian and calculating its mean and covariance matrix, one obtains

$$p(\mathbf{x}|\boldsymbol{\theta}_t, \boldsymbol{\theta}_d, \boldsymbol{\theta}_x, \mathbf{y}) = \delta(\mathbf{y}_0 - \mathbf{x}_0) \mathcal{N}(\mathbf{x}_1|\mathbf{x}_1^{\text{MAP}}, \sigma_e^2 \boldsymbol{\Phi}^{-1}) \delta(\mathbf{y}_2 - (\mathbf{x}_2 + \mathbf{v}_t)). \quad (31)$$

## VI. COMPUTATION OF THE CONDITIONAL DISTRIBUTIONS AND SAMPLING PROCEDURE

In this section, the conditional distributions which must be sampled from are explicitly computed, and the sampling procedure itself is detailed for each case. Since the initialization procedure for variables  $n_0$  and  $M$  is quite complicated, for the sake of organization, we first present it.

### A. Initialization procedure for $n_0$ and $M$

Experiments previously performed indicated that an accurate initialization of variables  $n_0$  and  $M$  was important for the effective convergence of the Gibbs sampler. Performing this initialization by hand (i.e., choosing the respective initial values by a visual inspection of the signal) may not be practical, and some method for automatically doing this task was required. An adaptation of the method for detection of long pulses in audio signals proposed in [8] was able to provide a quite accurate first estimate of the desired variables.

The initialization procedure looks for sudden high-amplitude impulses in time (typical of the initial discontinuity of the pulse), whose energy splits over the whole spectrum of a time frame around it. More precisely, the corrupted signal is split in contiguous blocks of length  $L$  with an overlap of 50% between adjacent blocks, and the discrete Fourier Transform

(DFT) [17] of each block is computed. Denote the DFT of block  $b$  by  $\hat{y}_b$ , for  $b = 1, \dots, B$ . Since typically the power of the audio spectrum is concentrated below some medium-high frequency, it is more convenient to look for unusual information in vectors  $\hat{y}_b$  above some frequency defined by the user. Denote this cut-off frequency by  $f_{co}$  and its respective frequency bin by  $\alpha_{co}$ . Define the function

$$\mu(b) = \frac{1}{\beta - \alpha_{co} + 1} \sum_{k=\alpha_{co}}^{\beta} |\hat{y}_b(k)|, \quad (32)$$

where  $\beta$  indexes the last bin in the DFT. This function is an arithmetic mean of the high-frequency content in block  $b$ , starting at frequency  $f_{co}$ . It is expected to reach a high value when the initial discontinuity of a pulse occurs in a given block of the degraded signal.

However, as reported in [8], if the considered signal exhibits a broad dynamic range with substantial high-frequency content (for example, brass or percussive instruments), the value of  $\mu$  can be high without necessarily implying the presence of long pulses. In order to circumvent this issue, here a median filter is applied to function  $\mu$ . As is known in the literature, the median filter is capable of removing local occurrences of unusual values within a sequence, and is widely used in Image Processing as a tool to remove impulsive noise while preserving edges [18]. The overall procedure is described below:

- Pad function  $\mu$  with  $\lfloor c/2 \rfloor$  zeros before its first and after its last samples, respectively.
- Define a new function  $\mu_m$  resulting of median filtering  $\mu$  with an odd-sized window of length  $c$ , that is, by replacing each value of  $\mu$  by the empirical median of the  $c$  values around it.
- Define function  $\Delta\mu(b)$  as the difference between  $\mu$  and  $\mu_m$  normalized by its highest value, that is,

$$\Delta\mu(b) = \frac{\mu(b) - \mu_m(b)}{\max_{b'} [\mu(b') - \mu_m(b')]}, \quad (33)$$

for  $b = 1, \dots, B$ . This ensures that the maximum absolute value of  $\Delta\mu$  is one, thus allowing an easier definition of the threshold specified below.

- Define a threshold  $\xi$  such that block  $b^*$  is considered corrupted by the initial discontinuity of a long pulse if  $|\Delta\mu(b^*)| \geq \xi$ .

This procedure defines a set of causally ordered candidate blocks  $b_1^*, \dots, b_M^*$ . Each contiguous subset of blocks  $b_i^*, \dots, b_j^*$  is attributed to the initial discontinuity of a long pulse, for which  $n_0$  is chosen as the first time sample of block  $b_i^*$ , and  $M$  as the gap size between the last time sample of block  $b_j^*$  and  $n_0$ .

In summary, in the initialization step the values of  $L$ ,  $f_{co}$ , and  $\xi$  are left to the user's choice. However, in order to reach a useful initialization, the value of  $L$ , representing the length of each block prior to the computation of its DFT, must be carefully chosen. For simplicity, all the block lengths here refer to a signal sampled at the frequency rate of 44,1 kHz. In [8] the authors adopted  $L = 2048$  ( $\approx 46$  ms). Since the portion of the signal being analyzed that contains the initial discontinuity

and the pulse tail typically spans around 10,000 samples ( $\approx 226$  ms), this choice of  $L$  would imply a crude time resolution, thus providing loose initial estimates for  $n_0$  and  $M$ . In order to increase time resolution, a value of  $L$  between 16 and 64 is suggested here. Experiments indicate that when the degraded signal is also contaminated with broadband additive noise, at low SNR, values of  $L$  near the upper-range allow for better estimates. Besides  $L \in \{16, 32, 64\}$ ,  $\xi = 0.4$  is recommended, and  $f_{co} = \frac{f'}{2}$  is a good starting point.

### B. Sampling $n_0$ and $M$

By using Bayes' Theorem and supposing prior independence between  $n_0$  and  $M$ , we have

$$p(n_0, M | \sigma_d^2, \theta_t, \mathbf{x}, \theta_x, \mathbf{y}) \propto p(\mathbf{y} | \theta_t, \theta_d, \theta_x, \mathbf{x}) p(n_0) p(M), \quad (34)$$

where  $p(\mathbf{y} | \theta_t, \theta_d, \theta_x, \mathbf{x})$  is given by Equation (22). Note that this equation depends implicitly on  $n_0$  and  $M$ , which influence the size of vectors  $\mathbf{y}_0$ ,  $\mathbf{y}_1$  and  $\mathbf{y}_2$ . Therefore, this formula defines a complicated distribution that is not easy to sample from, requiring a Metropolis-Hastings step within the Gibbs sampler for this purpose.

Firstly, we chose the prior distributions of  $n_0$  and  $M$  as uniform over the entire interval of samples being considered. Finally, the proposal distribution of the Metropolis-Hastings step is also uniform over an interval whose length can be controlled by the user, centered at their respective last sampled values.

### C. Sampling $\theta_t$ and $\mathbf{x}$

In order to sample from the joint posterior distribution of  $\theta_t$  and  $\mathbf{x}$  we recall the decomposition of  $p(\theta_t, \mathbf{x} | \theta_d, \theta_x, \mathbf{y})$  in Equation (17). By using Bayes' Theorem, it implies that this joint sampling is performed by first sampling  $\theta_t$  from  $p(\theta_t | \theta_d, \theta_x, \mathbf{y}) \propto p(\mathbf{y} | \theta_t, \theta_d, \theta_x) p(\theta_t)$  and then sampling  $\mathbf{x}$  from  $p(\mathbf{x} | \theta_t, \theta_d, \theta_x, \mathbf{y})$ .

The second step is quite straightforward, since this distribution was already computed and is given by Equation (31). Therefore, we only set  $\mathbf{x}_0 = \mathbf{y}_0$  and  $\mathbf{x}_2 = \mathbf{y}_2 - \mathbf{v}_t$ , and sample  $\mathbf{x}_1$  from a Gaussian distribution with mean  $\mathbf{x}_1^{\text{MAP}}$  and covariance matrix  $\sigma_e^2 \Phi^{-1}$ . Note that  $\mathbf{x}_1$  is initialized simply with zeros, meaning that no previous knowledge about the signal underlying the initial discontinuity is available.

The first step, sampling from  $p(\theta_t | \theta_d, \theta_x, \mathbf{y}) \propto p(\mathbf{y} | \theta_t, \theta_d, \theta_x) p(\theta_t)$  is more complicated, and depends on whether the shape-based or the Gaussian Process model is being considered. The former is briefly recalled below for the sake of completeness, followed by an exposition of the latter.

1) *Shape-based model:* Note that the distribution  $p(\theta_t^s | \theta_d, \theta_x, \mathbf{y}) \propto p(\mathbf{y} | \theta_t^s, \theta_d, \theta_x) p(\theta_t^s)$ , seen as a function of  $\theta_t^s$ , is very complicated, since  $p(\mathbf{y} | \theta_t^s, \theta_d, \theta_x)$  is given by Equation (26) and parameters in  $\theta_t^s$  influences it through  $\mathbf{y}_2$  and the model in Equation (6). Therefore, another Metropolis-Hastings step within the Gibbs sampler must be used to sample from it.

A possible choice of non-informative prior distribution  $p(\theta_t^s)$  are broad Gaussians for real-valued variables and Inverse Gamma with small parameters for the positive-valued

variables, in both cases assuming prior independence between components of  $\theta_t^s$ , as discussed in [7], [19]. The proposal distribution used in this Metropolis-Hastings step is a multivariate Gaussian centered on the previous accepted value of  $\theta_t^s$ , with diagonal covariance matrix whose terms are tuned by the user to keep the acceptance rate of this particular step around 50%, as suggested by some authors to guarantee that the sample space is well explored in a reasonable computational time [16].

2) *Gaussian Process model*: Recall that in this case  $\theta_t^G = [(\mathbf{v}_t^G)^T \sigma_f^2 \sigma_\ell^2]^T$ . Since we are adopting the Gaussian Process model in a Bayesian framework, it is possible to assign priors to the parameters of the covariance kernel  $\sigma_f^2$  and  $\sigma_\ell^2$  and estimate them together with the remaining variables. However, preliminary tests indicated that with a proper initialization, keeping these parameters constant during the whole procedure is enough to obtain a good estimate of the pulse with the Gibbs sampler, with the advantage of providing a decrease in the computational cost of the algorithm. The intuition behind this fact is that with a good initialization of variables  $n_0$  and  $M$ , guaranteed by the initialization procedure previously described, the overall shape of the pulse could be easily estimated, requiring only minor adjustments during the Gibbs sampler. Since parameters  $\sigma_f^2$  and  $\sigma_\ell^2$  are responsible for the overall shape of the pulse, they are not expected to change significantly during the entire procedure.

After initialization of variables  $n_0$  and  $M$ , we can consider the excerpt  $\mathbf{y}_2^{(0)}$  of the degraded signal after the initial estimate of the initial discontinuity. The pulse tail  $\mathbf{v}_t^G$ , along with parameters  $\sigma_f^2$  and  $\sigma_\ell^2$ , are then initialized by fitting a Gaussian Process with the squared-exponential kernel chosen for  $\mathbf{y}_2^{(0)}$ , via a standard maximum likelihood procedure [10]. Since the estimated values for  $\sigma_f^2$  and  $\sigma_\ell^2$  are kept constant, the only variable to be sampled in vector  $\theta_t^G$  is  $\mathbf{v}_t^G$ . By using Bayes' Theorem, we have that

$$p(\mathbf{v}_t^G | \theta_d, \theta_x, \mathbf{y}) \propto p(\mathbf{y} | \mathbf{v}_t^G, \theta_d, \theta_x) p(\mathbf{v}_t^G), \quad (35)$$

where  $p(\mathbf{y} | \mathbf{v}_t^G, \theta_d, \theta_x)$  has already been determined in Equations (26) and (27), further simplified as Equations (28) and (29). Since we are supposing that  $\mathbf{v}_t^G$  is well described by a Gaussian Process with a squared-exponential covariance kernel, we have that  $p(\mathbf{v}_t^G) \sim \mathcal{N}(\mathbf{0}, \mathbf{C})$ , where matrix  $\mathbf{C}$  is given by the Gram matrix of the covariance kernel function, computed from Equation (9). Therefore, the conditional posterior distribution for  $\mathbf{v}_t^G$  is given by

$$p(\mathbf{v}_t^G | \theta_d, \theta_x, \mathbf{y}) \propto \exp\left(-\frac{1}{2}(\mathbf{v}_t^G)^T \mathbf{C} \mathbf{v}_t^G\right) \exp\left(-\frac{1}{2} \mathbf{z}^T \mathbf{R} \mathbf{z}\right) = \exp\left\{-\frac{1}{2}((\mathbf{v}_t^G)^T \mathbf{C} \mathbf{v}_t^G + \mathbf{z}^T \mathbf{R} \mathbf{z})\right\}. \quad (36)$$

We must then compute the term  $\mathbf{z}^T \mathbf{R} \mathbf{z}$  in order to make explicit its dependence on  $\mathbf{v}_t^G$ . To this end, note that it can be

rewritten as:

$$\begin{aligned} \mathbf{z}^T \mathbf{R} \mathbf{z} &= [\mathbf{y}_0^T \ (\mathbf{y}_2 - \mathbf{v}_t^G)^T] \begin{bmatrix} \mathbf{R}_{11} & \mathbf{R}_{12} \\ \mathbf{R}_{21} & \mathbf{R}_{22} \end{bmatrix} \begin{bmatrix} \mathbf{y}_0 \\ \mathbf{y}_2 - \mathbf{v}_t^G \end{bmatrix} = \\ &= \mathbf{y}_0^T \mathbf{R}_{12} \mathbf{v}_t^G - (\mathbf{v}_t^G)^T \mathbf{R}_{21} \mathbf{y}_0 - \mathbf{y}_2^T \mathbf{R}_{22} \mathbf{v}_t^G \\ &= (\mathbf{v}_t^G)^T \mathbf{R}_{22} \mathbf{y}_2 + (\mathbf{v}_t^G)^T \mathbf{R}_{22} \mathbf{v}_t^G \\ &+ \text{terms not depending on } \mathbf{v}_t^G. \end{aligned} \quad (37)$$

Therefore, we have that

$$\begin{aligned} (\mathbf{v}_t^G)^T \mathbf{C} \mathbf{v}_t^G + \mathbf{z}^T \mathbf{R} \mathbf{z} &= \\ &= \mathbf{y}_0^T \mathbf{R}_{12} \mathbf{v}_t^G - (\mathbf{v}_t^G)^T \mathbf{R}_{21} \mathbf{y}_0 - \mathbf{y}_2^T \mathbf{R}_{22} \mathbf{v}_t^G \\ &= (\mathbf{v}_t^G)^T \mathbf{R}_{22} \mathbf{y}_2 + (\mathbf{v}_t^G)^T \mathbf{R}_{22} \mathbf{v}_t^G + (\mathbf{v}_t^G)^T \mathbf{C} \mathbf{v}_t^G \\ &+ \text{terms not depending on } \mathbf{v}_t^G. \end{aligned} \quad (38)$$

Since this expression is quadratic in  $\mathbf{v}_t^G$ , the conditional posterior distribution for  $\mathbf{v}_t^G$  is a Gaussian whose mean vector and covariance matrix can be easily computed by completing the squares on the expression above, as indicated in the beginning of Section V. We then have that  $p(\mathbf{v}_t^G | \theta_d, \theta_x, \mathbf{y}) = \mathcal{N}(\mathbf{v}_{t,\text{mean}}^G, \Sigma)$ , where

$$\begin{aligned} \mathbf{v}_{t,\text{mean}}^G &= [\mathbf{R}_{22} + \mathbf{R}_{22}^T + \mathbf{C}^{-1} + \mathbf{C}^{-T}]^{-1} \times \\ & \quad [(\mathbf{R}_{12}^T + \mathbf{R}_{21}) \mathbf{y}_0 + (\mathbf{R}_{22}^T + \mathbf{R}_{22}) \mathbf{y}_2] \end{aligned} \quad (39)$$

$$\Sigma = \left[ \frac{1}{2} (\mathbf{R}_{22} + \mathbf{R}_{22}^T + \mathbf{C}^{-1} + \mathbf{C}^{-T}) \right]^{-1}. \quad (40)$$

We now impose two additional simplifications:

- Since the tail of the pulse varies much slower than the original underlying signal we can abandon its AR structure, at least in the region of the pulse tail. This corresponds to considering matrix  $\mathbf{A}_2$  as an identity matrix, and then matrix  $\mathbf{R}_{22}$  turns out to be diagonal with constant terms. Intuitively, we are considering that the underlying original signal is essentially white noise when compared to the tail of the pulse.
- Sampling from the distribution  $\mathcal{N}(\mathbf{v}_{t,\text{mean}}^G, \Sigma)$  is very expensive, since the size of  $\mathbf{v}_t^G$  can be of the order of thousands of time samples. Therefore, instead of sampling from it, at each step of the algorithm we simply compute its mean  $\mathbf{v}_{t,\text{mean}}^G$  and consider its value as the current value of  $\mathbf{v}_t^G$ .

Finally, note that if we have two overlapping pulses, their respective tails are being modeled by Gaussian Processes, and when the respective tails overlap, its distribution will still be Gaussian. Therefore, this modeling may allow a simpler treatment of this heretofore complicated scenario. However, preliminary tests indicated that the estimation of the AR model parameters in order to interpolate the signal underlying an initial discontinuity superimposed to an unfinished pulse tail is problematic; this issue is left to be addressed in a future work.

#### D. Sampling $\sigma_d^2$

This is the last step of the Gibbs sampler. To compute the required posterior distribution, we use Bayes' Theorem once again and obtain

$$p(\sigma_d^2 | n_0, M, \boldsymbol{\theta}_t, \mathbf{x}, \boldsymbol{\theta}_x, \mathbf{y}) \propto p(\mathbf{y} | \boldsymbol{\theta}_t, \boldsymbol{\theta}_d, \boldsymbol{\theta}_x, \mathbf{x}) p(\sigma_d^2). \quad (41)$$

Now, the dependence of  $p(\mathbf{y} | \boldsymbol{\theta}_t, \boldsymbol{\theta}_d, \boldsymbol{\theta}_x, \mathbf{x})$  on  $\sigma_d^2$  is very simple: as can be seen in Equation (22), it is just a scale parameter for the distribution. Therefore, the Inverse Gamma distribution with parameters  $\alpha_d$  and  $\beta_d$  is a good choice of prior distribution, since it implies that  $p(\sigma_d^2 | n_0, M, \boldsymbol{\theta}_t, \mathbf{x}, \boldsymbol{\theta}_x, \mathbf{y})$  is also an Inverse Gamma with parameters given by

$$\alpha = \alpha_d + \frac{M}{2} \quad (42)$$

and

$$\beta = \beta_d + \frac{1}{2} \sum_{i=0}^{M-1} \mathbf{v}_d(n_0 + i)^2. \quad (43)$$

Hyperparameters  $\alpha_d$  and  $\beta_d$  are chosen very close to zero to turn the prior vague, reflecting no previous knowledge about  $\sigma_d^2$ .

## VII. RESULTS

The performance of the proposed algorithm was evaluated through tests performed in two distinct scenarios: (A) a real signal artificially distorted by pulses following Equation 6; and (B) two real degraded signals. The former allows us to assess the method's accuracy and convergence, and compare its performance against previous results; the latter informs us about the method's capability of dealing with real distortions. The tests were run in a personal computer with a quadcore processor operating at 1.60 GHz clock and 8 GB of RAM. All signals are monophonic, sampled at 44.1 kHz with 16-bit precision, and implementations are in MATLAB<sup>TM1</sup>.

Only results of the Gaussian Process modeling of the pulse are shown, since its perceived quality is nearly the same as that of the shape-based one, while the convergence of the latter is much more problematic for naturally degraded signals. Results related to the shape-based model are further discussed in [7], [19].

#### A. Real signal, artificially degraded

The chosen signal is an 8-second long excerpt of jazz quartet music with drums, bass, guitar and clarinet, degraded by eleven severe non-overlapping and uniformly spaced pulses following Equation 6.

The whole signal was given as input to the initialization procedure, with parameters  $L = 16$ ,  $\xi = 0.3$ ,  $c = 5$  and  $f_{co} = 3$  kHz, and its output, function  $\Delta\mu$ , is shown in Figure 2, which shows that all pulses are correctly identified. Afterwards, an excerpt of size  $N = 8,000$  samples containing each pulse was separately processed. Within each block, the initial estimate of  $n_0$  was fixed at 500, and the parameters of the order-40 AR model used to infer the underlying signal

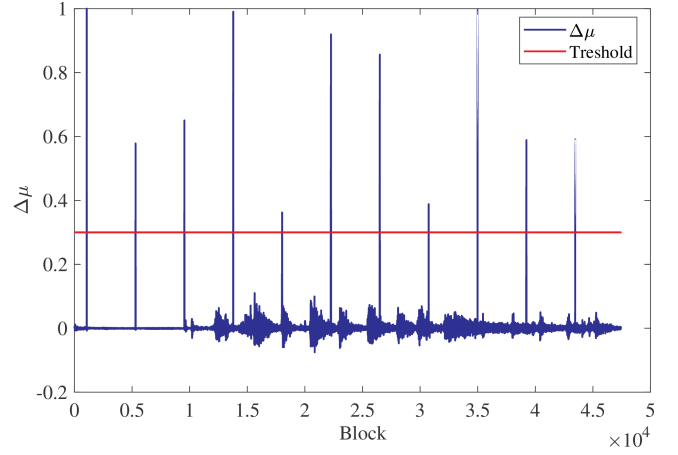


Fig. 2. Function  $\Delta\mu$  – output of the initialization procedure.

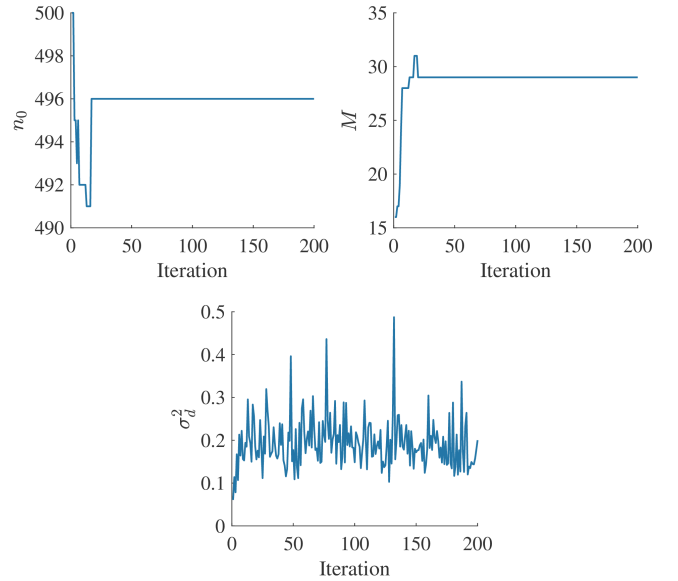


Fig. 3. MCMC sampled values for  $n_0$ ,  $M$  and  $\sigma_d^2$  for the first pulse.

in the initial discontinuity were estimated based on the first 450 samples in the block. To guarantee enough proximity to the stationary distribution, 200 iterations of the Gibbs sampler were run for each pulse, being the first 150 discarded as burn-in time. Each iteration lasted for approximately 15 s.

Figure 3 shows the convergence of  $n_0$ ,  $M$  and  $\sigma_d^2$  for the first pulse of this signal. It can be seen that the conditional posterior distributions for  $n_0$  and  $M$  are highly concentrated around a single value. Such behavior is expected in this scenario since the artificial degradation was introduced in a signal without other defects, such as broadband additive noise and clicks, which can cause the variance of these distributions to increase. Similar behavior was observed for the other pulses present within this signal. Therefore, the proposed method was shown to be capable of provide a good initial estimate for  $n_0$  and  $M$ , and refine them in few iterations.

Figure 4 compares the degraded signal (thin solid line) and estimated pulse (thick dashed line) for the same pulse, illustrating that the Gaussian Process model for the tail of

<sup>1</sup>The MathWorks, Inc., <http://www.mathworks.com/>.

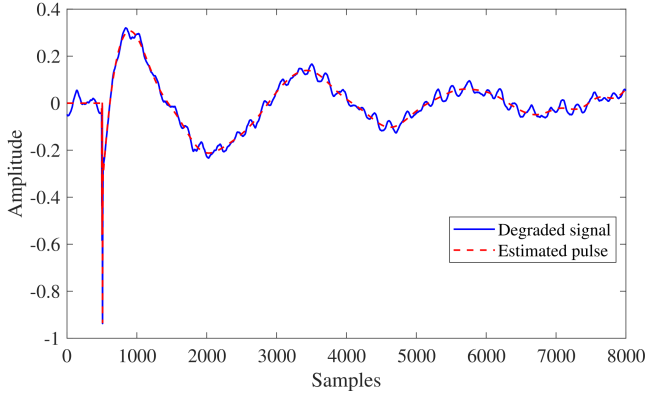


Fig. 4. Degraded signal (thin solid line) and estimated pulse (thick dashed line) for the first pulse.

TABLE I

PEAQ GRADES FOR THE REAL SIGNAL ARTIFICIALLY DEGRADED AND ITS RESPECTIVE RESTORED VERSIONS. THE CLOSER THE GRADE IS TO ZERO, THE CLEANER THE SIGNAL.

Signal	PEAQ grade
Distorted	-1.5287
Proposed algorithm	-0.1487
TPSW	-0.2359
AR	-0.3345

the pulse is capable of correctly identifying it, even with the stationary squared-exponential covariance kernel.

In order to objectively assess the quality of the restored signal, we evaluated it through the PEAQ (Perceptual Evaluation of Audio Quality) [20], [21] algorithm, tailored to compare the perceived quality of a wideband audio signal against a reference signal after mapping them to a perceptual domain that models the operation of the human auditory system. The output score is a number from 0 (imperceptible difference from the reference signal) to -4 (very annoying differences). Table I compares the proposed method with [5], based on the TPSW filtering, and [4], based on the AR separation technique. As required by the PEAQ algorithm, signals were previously upsampled to 48 kHz.

Note that the proposed algorithm yields a signal with marginally better PEAQ score than its competitors. In practice, these numbers mean that the three restored signals sound almost identical, a fact that was verified by informal listening tests. However, our proposed algorithm automatically locates the initial discontinuity and its duration, improves these initial estimates and interpolates the underlying signal; in addition, it produces a very accurate estimate of the pulse tail using the Gaussian Process model. Even so, it requires significantly less user intervention than the other two, since it has only a few parameters to be set.

### B. Real degraded signals

The two signals considered in this scenario are: an excerpt of 3 seconds from cylinder recording number 154 from [22], approximately from 1907, containing a severe pulse at the beginning when the music that will be played is introduced;

TABLE II  
PARAMETERS OF THE INITIALIZATION PROCEDURE FOR THE CYLINDER AND CHOPIN SIGNALS.

Parameter	Signal	
	Cylinder	Chopin
$L$	64	64
$\xi$	0.4	0.3
$c$	31	7
$f_{co}$	10,000	3,000

and an excerpt of 11 seconds from a piece by Chopin for solo piano, containing six pulses. Both are sampled at 44.1 kHz with 16-bit resolution. Parameters of the initialization procedure for each signal are shown in Table II. They were manually tuned in order to correctly identify the pulses only, and not other defects also present within the signal, such as clicks and crackles. Essentially, signals with more background noise requires a higher value of  $f_{co}$  and  $c$ , but since the initialization procedure is very fast, lasting less than 1 s, some trial and error is not tedious or time-consuming. In both cases, since the tail of the pulse is not too long, an excerpt of only 2,000 samples containing the degradation was processed. The Gibbs sampler ran for 500 iterations and the first 400 ones were discarded. Each iteration lasted for approximately 0.5 s.

Since in this scenario we do not have a reference signal, it is not possible to compute the PEAQ grade, so we will present a brief discussion about the restoration on both cases:

- In the cylinder excerpt, the restoration seems almost perfect. A very light click remains where the pulse originally started, although almost masked by the high background noise present throughout the signal. On the other hand, there is no vestige of the low-frequency content of the pulse tail.
- In the Chopin excerpt, the remnant of the initial discontinuities, this time in the form of a short-duration and low-level hiss, is more apparent because of the lower level of background noise in the signal. However, once more there is also no perceptible vestige of the low-frequency content of the pulse in the restored signal.

This small residue left after the interpolation of the signal underlying the initial discontinuity is much probably due to the impairment of the AR modeling by the presence of background noise, as discussed in [3]. This issue could be worked around by including the estimation of its parameters in the Gibbs sampler, instead of keeping them constant. However, the high impact on the overall computational load found in preliminary tests suggested that the simplified approach should be adopted and that this point should be further investigated with a view to a new version of the algorithm. However, it should be stressed that, as in the controlled experiments, the proposed algorithm was shown to be capable of identifying the location and extent of the initial discontinuity as well as the tail of the pulse when dealing with real degraded signals, a much more challenging scenario where defects other than the long pulses may also be present.

## VIII. CONCLUSION

In this paper we presented a novel algorithm for the restoration of audio signals degraded by long pulses with significant low-frequency content that circumvents two main drawbacks of previous works: a large quantity of hyper-parameters difficult to interpret that must be adjusted manually, and the need to know the location of the pulse beforehand. These issues were addressed through modeling of the pulse tail via Gaussian Process and a Bayesian framework that includes location as a random quantity to be estimated. The signal underlying the initial discontinuity is also interpolated along the procedure. In order to accelerate the convergence of the Gibbs sampler, we employed an efficient initialization algorithm based on the time-frequency content of the degraded signal that roughly locate the beginning of the degradation. In controlled experiments, when compared to previous approaches our algorithm shows a slightly better performance, according to the PEAQ grades. These results are confirmed by the experiments with real degraded signals.

Some improvements to the proposed algorithm will be addressed in future works: 1) make it able to handle overlapping pulses; and 2) refine the restored signal interpolation in the region of the initial discontinuity, which is likely to be impaired by other degradations such as background noise. Both points are linked to the difficulty of estimating the AR model parameters and further interpolate the restored signal in the region of the discontinuities in noisy scenarios; this is the next research target.

Another possible improvement is to sub-sample the pulse tail before the Gibbs sampler. This will significantly decrease the computational cost of the algorithm, since at each iteration a matrix of size approximately  $N \times N$  must be inverted. The sub-sampling can be justified by the fact that it implies no relevant loss of information on the tail, since it usually contains much lower frequencies than the typical underlying signal.

## REFERENCES

- [1] S. V. Vaseghi, "Algorithms for restoration of archived gramophone recordings," Ph.D. Thesis, University of Cambridge, Cambridge, UK, 1988.
- [2] S. V. Vaseghi and R. Frayling-Cork, "Restoration of old gramophone recordings," *Journal of the Audio Engineering Society*, vol. 40, no. 10, pp. 791–801, 1991.
- [3] S. J. Godsill and P. J. W. Rayner, *Digital Audio Restoration - A Statistical Model Based Approach*. Cambridge, UK: Cambridge University Press, 1998.
- [4] S. J. Godsill and C. H. Tan, "Removal of low frequency transient noise from old recordings using model-based signal separation techniques," in *Proceedings of the IEEE Workshop on Applications of Signal Processing to Audio and Acoustics (WASPAA 1997)*. New Paltz, USA: IEEE, October 1997.
- [5] P. A. A. Esquef, L. W. P. Biscainho, and V. Välimäki, "An efficient algorithm for the restoration of audio signals corrupted with low-frequency pulses," *Journal of the Audio Engineering Society*, vol. 51, no. 6, pp. 502–517, 2003.
- [6] P. A. A. Esquef and G. S. Welter, "Audio de-thumping using Huang's empirical mode decomposition," in *Proceedings of the 14th. International Conference on Digital Audio Effects (DAFx-11)*, Paris, France, September 2011.
- [7] H. T. Carvalho, F. R. Ávila, and L. W. P. Biscainho, "A Bayesian procedure for restoration of audio signals degraded by low-frequency pulses," in *Proceedings of the 12th. Brazilian Conference on Audio Engineering*. São Paulo, Brazil: AES-Brazil, May 2014, pp. 47–54.
- [8] P. A. A. Esquef, L. W. P. Biscainho, and P. S. R. Diniz, "Detecção de pulsos longos em sinais de áudio," in *Proceedings of the XVII Brazilian Symposium on Telecommunications (SBTr)*. Vila Velha, Brazil: SBTr, September 1999, pp. 191–196, in Portuguese.
- [9] C. M. Bishop, *Pattern Recognition and Machine Learning*. New York, USA: Springer, 2007.
- [10] C. E. Rasmussen and C. K. I. Williams, *Gaussian Processes for Machine Learning*, 1st ed. Cambridge, USA: MIT Press, 2006.
- [11] D. J. C. MacKay, *Information Theory, Inference and Learning Algorithms*, 1st ed. Cambridge, UK: Cambridge University Press, 2003.
- [12] A. G. Wilson, "Covariance kernels for fast automatic pattern discovery and extrapolation with gaussian processes," D.Sc. Thesis, University of Cambridge, Cambridge, UK, 2014.
- [13] S. Geman and D. Geman, "Stochastic relaxation, Gibbs distributions, and the Bayesian restoration of images," *IEEE Transactions on Pattern Analysis and Machine Intelligence*, vol. 6, no. 6, pp. 721–741, 1984.
- [14] C. Robert and G. Casella, *Introducing Monte Carlo Methods with R*, 1st ed. New York, USA: Springer, 2009.
- [15] —, *Monte Carlo Statistical Methods*, 2nd ed. New York, USA: Springer, 2005.
- [16] G. H. Givens and J. A. Hoeting, *Computational Statistics*, 2nd ed. Hoboken, USA: Wiley, 2012.
- [17] A. V. Oppenheim and R. W. Schaffer, *Discrete-Time Signal Processing*, 3rd ed. Upper Saddle River, USA: Prentice Hall, 2009.
- [18] A. K. Jain, *Fundamentals of Digital Image Processing*, 1st ed. Upper Saddle River, USA: Pearson, 1988.
- [19] H. T. Carvalho, "Bayes meets bach: Applications of bayesian statistics to audio restoration," D.Sc. Thesis, Universidade Federal do Rio de Janeiro, Rio de Janeiro, Brazil, 2017.
- [20] ITU-R, *Rec. BS.1387-1: Method for Objective Measurements of Perceived Audio Quality*. Geneva, Switzerland: International Telecommunication Union, 2001.
- [21] P. Kabal, "An examination and interpretation of ITU-R BS.1387: Perceptual evaluation of audio quality," McGill University, Montreal, Canada, In: Report 217, 2002.
- [22] B. de Catalunya, "Uns incunables del sonor - la collecció regordosaturull de cilindres de cera," <http://www.bnc.cat/Exposicions/Uns-incunables-del-sonor/Continguts-de-l-exposicio>.